

REPORT FHWA/NY/SR-04/141

# In-Service Performance of an FRP Superstructure

SREENIVAS ALAMPALLI  
GEORGE SCHONGAR  
HARRY GREENBERG



**SPECIAL REPORT 141**  
**TRANSPORTATION RESEARCH AND DEVELOPMENT BUREAU**  
**NEW YORK STATE DEPARTMENT OF TRANSPORTATION**  
George E Pataki, Governor/Joseph H. Boardman, Commissioner



# **IN-SERVICE PERFORMANCE OF AN FRP SUPERSTRUCTURE**

Sreenivas Alampalli, Director, Bridge Program and Evaluation Services Bureau  
George Schongar, Civil Engineer I, Transportation R&D Bureau  
Harry Greenberg, Lab Equipment Designer, Transportation R&D Bureau

Special Report 141  
March 2004

TRANSPORTATION RESEARCH AND DEVELOPMENT BUREAU  
New York State Department of Transportation, State Campus, Albany, New York 12232



## **ABSTRACT**

The first fiber reinforced polymer composite bridge superstructure in New York State was installed in late 1998. These materials are new to bridge applications, therefore no data exists on their in-service performance. A detailed test program of periodic testing and visual inspections was used to monitor its in-service performance, characterize its dynamic properties, and obtain data to calibrate theoretical analyses. This report documents the test program and summarizes the results. The test data indicate that the superstructure is structurally performing well. Several delaminations were found during visual inspections and wearing surface was replaced once. For future applicability of these materials for such applications, these issues affecting the long-term durability of FRP bridge decks should be resolved.



## **CONTENTS**

<b>I. INTRODUCTION</b> .....	1
<b>II. BRIDGE STRUCTURE</b> .....	3
<b>III. IN-SERVICE MONITORING</b> .....	5
A. INSTRUMENTATION .....	5
B. INITIAL PROOF-LOAD TEST .....	7
C. FOLLOW-UP LOAD TESTS .....	10
D. IMPACT FACTORS .....	15
E. DYNAMIC CHARACTERISTICS .....	15
F. VISUAL INSPECTION .....	20
<b>IV. CONCLUSIONS</b> .....	23
<b>ACKNOWLEDGMENTS</b> .....	25
<b>REFERENCES</b> .....	27





## I. INTRODUCTION

Fiber-reinforced polymer (FRP) materials are a viable alternative for replacing short-span concrete slab bridges. Since most components are shop-fabricated, the on-site time required for construction can be reduced significantly for small bridges. In late 1998, New York State Department of Transportation (NYSDOT) replaced a deteriorated bridge superstructure using a fiber reinforced slab in significantly less time than a conventional bridge project (see Figure 1). This was the first FRP superstructure in the United States on a Federal Highway Administration (FHWA) recognized state highway. A previous report (*1*) documented the FRP slab design, fabrication, installation, proof-testing, long-term monitoring, and cost-benefit details. The in-service performance of the bridge was monitored for nearly four years through periodic load testing and visual inspection. Modal tests were conducted to characterize its dynamic properties, and to calibrate theoretical analyses. A detailed finite element analysis was then used to further investigate its failure mechanisms and to optimize future designs. This report describes the field inspection and experimental investigations.



**Figure 1. FRP superstructure.**



## II. BRIDGE STRUCTURE

The FRP superstructure (Figure 1) is part of the state owned bridge crossing Bennetts' Creek, just south of Rexville, NY. It is 7.8-m long, 10-m wide, and has a 30 degree skew. The superstructure is fabricated from an E-glass-stitched bonded fabric and vinyl ester resin using a cell core system that provides stiffness in two directions. It has a depth of 621 mm with a 10-mm thick polymer-concrete wearing surface. It was fabricated in two skewed pieces, each 5.036-m wide and 7.807-m long, with a longitudinal joint along the centerline of the bridge (see Figure 2). The joint is designed to carry the shear that develops along the plane resulting from the differential deflection of the two superstructure panels. The shear at the joint is resisted through a combination of a mechanical key-way and a resin glue. The railings on the structure are two steel box beams attached to a vertical faced concrete parapet that used FRP facing panels as stay-in-place forms. Additionally, conventional steel-reinforcing bars were embedded in the FRP deck and extend into the concrete filled barriers. Both ends of the bridge are fixed against movement. It was anchored to the abutment by 25-mm stainless steel anchor bolts that were drilled through the superstructure and bearing pad into the concrete bridge seat and then grouted in-place. Recesses for the anchors were filled with a non-shrink grout. The fabrication, design, and construction details are documented in an earlier report (1).



Figure 2. FRP superstructure's longitudinal shear-key.

The FRP superstructure is designed for the AASHTO MS 23 live load (2). The maximum strain on the composite material was limited to 20% of ultimate under service loads with live load deflection limited to the span length divided by 800 (8.76 mm in this case). A dead load allowance for a 50 mm future wearing surface was made. The estimated inventory load rating (I, 3) is MS-120 (114 Metric Tons) and the operating rating is MS-160 (286 Metric Tons). Since the design is controlled by deflection criteria, both the computed inventory and operating ratings are very high.

### **III. IN-SERVICE MONITORING**

The bridge was instrumented and a proof-load test was conducted before the structure was opened to traffic. This was done to ensure the structure's integrity before opening it to the public, to establish base line conditions for a future monitoring program, and to compare actual performance with theoretical calculations. After the initial proof-test was conducted, the load tests were repeated periodically to ensure that the structure was behaving satisfactorily and to look for any signs of degradation. These tests were also used to estimate the impact factors. Modal tests were conducted to characterize its dynamic properties in terms of modal frequencies and damping ratios.

#### **A. INSTRUMENTATION**

The superstructure was instrumented with 24 conventional strain gauges mounted externally on the bottom face skin of the superstructure. The locations of the strain gages are shown in Figure 3. All the strain gages were of Type EA-06-250AF-120-general purpose, 120  $\Omega$ , self-temperature compensating, constantan foil strain gages, manufactured by Micro Measurements Group. All the gages were made watertight and protected from the environment for long-term monitoring use. A general purpose strain gage measurement system was employed for data acquisition.

Eighteen gages were mounted in the longitudinal direction, six at the centerline on either side of the shear key, three at each quarter point and three at each end. Six gages were mounted transversely at the centerline of the bridge, two near the midspan, two at quarter span, and two near beam supports (see Figure 3). These locations were chosen to investigate strains at the span midpoints and quarter points. Gages placed along the centerline shear key check strain compatibility across the longitudinal joint. Gages were also placed transversely to investigate the load distribution characteristics of the structure.

Survey measurements were used to monitor the midspan deflections of the slab during the initial proof load test. During two of the subsequent tests, in April and November of year 2000, six LVDTs (Type GHSD 750-500 manufactured by Macro Sensors) were used to measure the deck deflection and load transfer across the shear key (Figure 4). They were mounted on a wood beam that spanned the length of the bridge set below the deck. The beam was supported on the abutments on both sides. The LVDTs were mounted on the south side of the bridge on either side of the shear key at the centerline, quarter point, and 200 mm from the abutment wall.

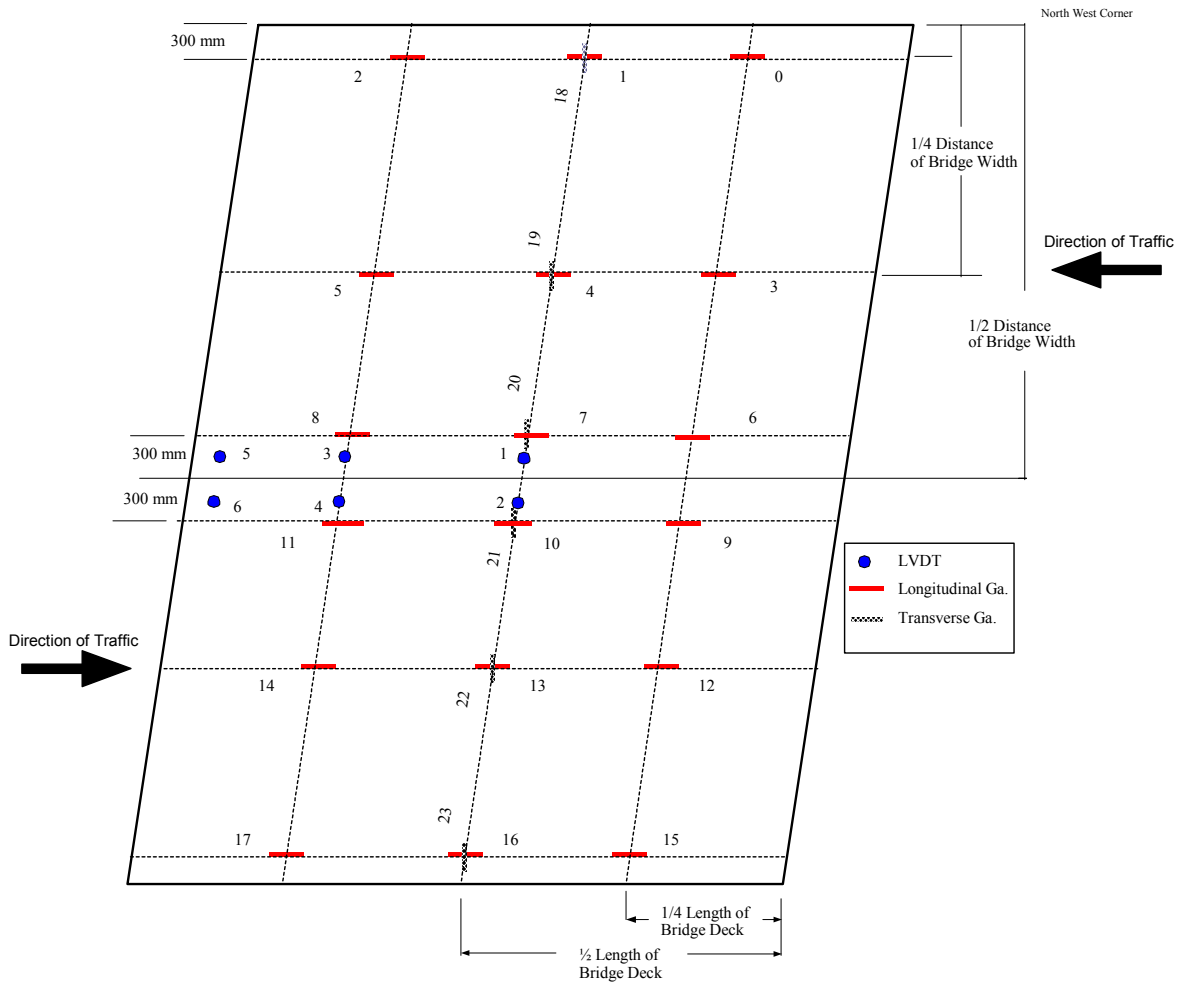


**Figure 3. Location of strain gages and LVDTs.**

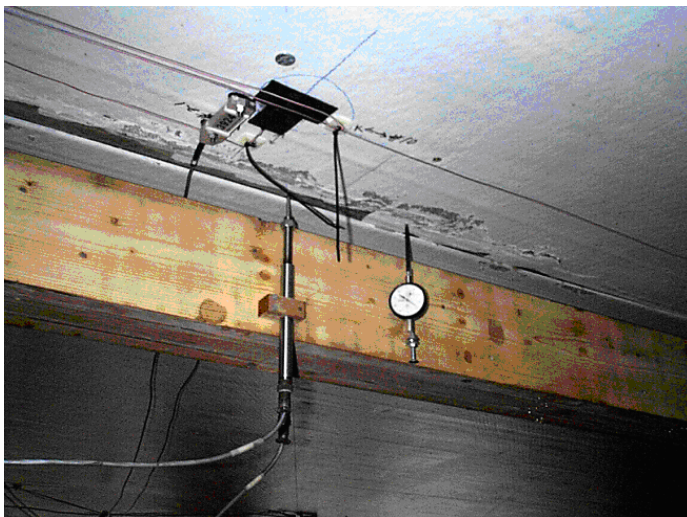


**Figure 4. LVDT for deflection measurement.**

In 2001, experimental modal analysis techniques were used to characterize the dynamic behavior of the structure in terms of its modal parameters (natural frequencies, damping ratios, and mode shapes). An impact test setup was used, where the bridge response was measured at a single location while excitation was induced at number of locations on the superstructure. An impulse hammer (PCB Model 086B50 with a built-in load cell to measure the induced force) was used to excite the bridge (Figure 1) and an accelerometer (PCB Flexcel Model 336A04 with 100-mV/g sensitivity) was used to measure the bridge response. The accelerometer was mounted to the bridge with modal wax. Only vertical vibration response perpendicular to the plane of the composite deck was measured. A Tektronix four-channel dynamic signal analyzer (Model 2630) obtained time-domain and frequency-domain data required for the analysis.

## B. INITIAL PROOF-LOAD TEST

Proof load tests establish inventory and operating ratings for bridges using a test operating factor (1.4 in this case). A target proof load was employed to load the bridge beyond the design load (4). Four ten-wheel, loaded dump trucks were used during the test (see Figure 5). Each of these trucks closely resemble AASHTO M-18 Truck configuration (2). They were loaded to capacity and weighed on-site with portable truck scales. Although the target proof load could not be reached due to truck size and load limitations, MS 23 loadings were achieved (Table 1).

**Table 1. Comparison of test loads with proof-load and MS23 load.**

	MS23	Target Proof-Load	Actual Test-Load
Moment (kN-m)	624	873	755
Shear (kN)	495	693	486

Four different load cases were used, so that the load could be increased in increments, as follows: Case 1: Two Empty Trucks, Case 2: Two Loaded Trucks (Normal Load), Case 3: Four Loaded Trucks (Normal Load), and Case 4: Four Loaded Trucks (Overload). Case 4 was the proof-load condition. The trucks were placed at pre-marked positions on the bridge to maximize bending moments. Each truck was moved on and off the bridge individually for each load case and data was recorded at each step. For the cases involving four trucks, the trucks in each lane were placed back to back (see Fig. 5). The strain data for Case 4 are given in Figure 6 and Table 2.





**Figure 5. Proof-testing of the FRP Superstructure.**

### Maximum Strains

The data from the load cases is generally consistent in the sequence and symmetry of the loading. The data also tends to show generally lower strains in the southeast portion of the bridge (gages 11, 14, and 17) than corresponding gages in other quadrants. This may be attributed to a greater fixity of the superstructure to substructure connection in the southeast quadrant due to variations in drilling and grouting of the anchor bolts during construction.

The maximum strain recorded was considerably less than the approximately  $600 \mu\epsilon$  predicted by the analysis conducted by the manufacturer (see Figure 6 and Table 2). This indicates a significantly higher load capacity than that originally assumed (3). The maximum deflection at mid-span during Case 4 was measured to be less than 3.5 mm, which is considerably less than the  $\text{Span}(L)/800$  design limitation of 8.8 mm.

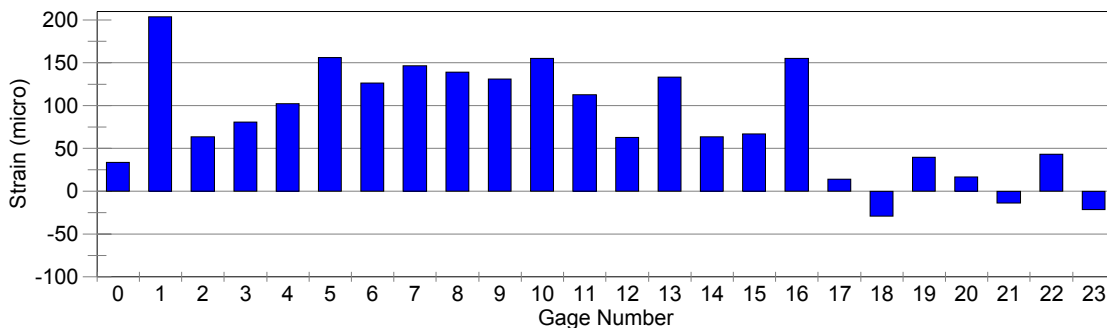


**Figure 6. Strain data under proof load (see Figure 3 for gage locations).**



**Table 2. Strain data under proof load.**

Gage	Strain( $\mu\epsilon$ )	Gage	Strain( $\mu\epsilon$ )	Gage	Strain( $\mu\epsilon$ )	Gage	Strain( $\mu\epsilon$ )
0	33	6	127	12	62	18	-30
1	204	7	147	13	134	19	40
2	67	8	139	14	64	20	17
3	81	9	132	15	67	21	-14
4	102	10	156	16	156	22	44
5	157	11	113	17	14	23	-22

### Shear-Key Performance

As indicated in the previous section, there is a longitudinal joint along the centerline of the bridge that was designed to carry the shear developed along the plane resulting from the differential deflection of the two superstructure panels. The shear at the joint is resisted through a combination of a mechanical key-way and a resin glue. If the shear-key system behaves as intended, then the strains experienced by the gages on both sides of the joint should be nearly the same.

An examination of the data (from Case 4) from the gages located along the centerline showed generally consistent results between adjacent pairs of gages located across the centerline longitudinal joint (see Figure 7 and Table 3). Based on this, it can be concluded that the loads were being effectively transferred across the centerline longitudinal shear key.

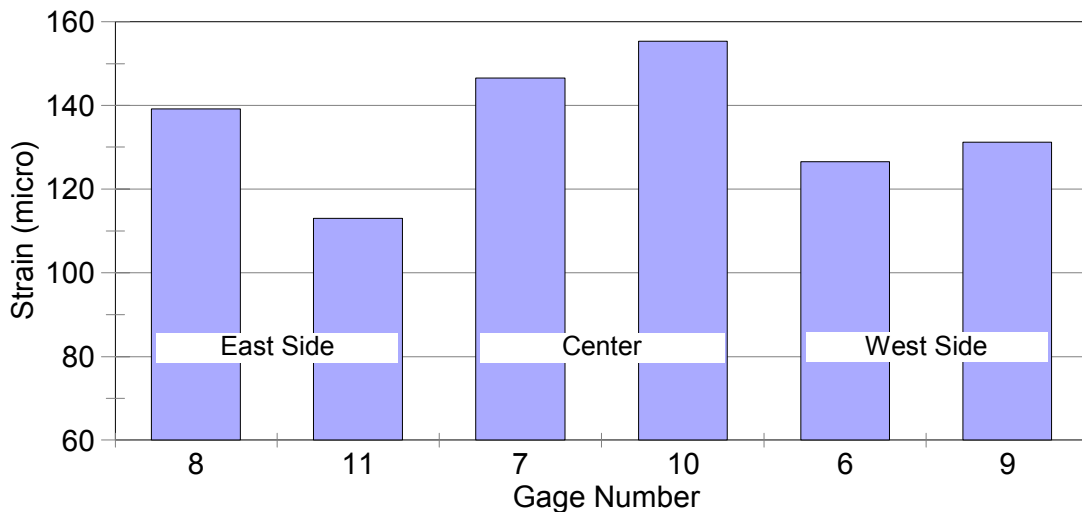


**Figure 7. Strains from gages on both sides of the shear-key.**

**Table 3. Strains from gages on either side of the shear-key under proof-load.**

Gage	8	11	7	10	6	9
Strain( $\mu\epsilon$ )	139	113	146	156	127	132

### C. FOLLOW-UP LOAD TESTS

The first proof test conducted soon after the FRP deck was opened to traffic, as described in the previous section, established the reference/baseline for future bridge monitoring through similar load testing. The superstructure was tested periodically for four years to study its in-service durability. This section gives test details and results.

The initial proof-load tests was conducted during October 1998. Follow-up tests were conducted at six-month intervals in May 1999, November 1999, April 2000, November 2000, and September 2002. These tests utilized only Load Case 4, where four loaded trucks were utilized (two trucks in each lane with the trucks in each lane placed back to back) as shown in Figure 5, except for the test conducted in November 1999. In November 1999, due to winter maintenance operations trucks were fitted with snow-plowing blades. This made it impossible to place four trucks one time on the bridge, and hence the load test utilized only two trucks placed back to back (one in each lane), maximizing the moment at center of the superstructure. The truck weights are shown in Table 4, and the corresponding results in Figures 8-9 and Tables 5-6. Note that all the strain data has been normalized to the proof-load utilized in the baseline test for comparison. The performance of shear-key was evaluated using the gages placed adjacent to the shear-key, and are summarized in Figure 10 and Table 7.

The results indicate that the strain data from subsequent tests compare well to the initial proof-load test data, indicating that the FRP slab bridge is performing well in-service as expected without any structural problems. The data also indicate that the shear-key is performing well. The same conclusion was reached using LVDTs placed along the centerline (Figures 11-12 and Tables 8-9).

**Table 4. Weights of the trucks used in load tests.**

Test Date	Truck	Driver Side Center Axle	Driver Side Rear Axle	Passenger Side Center Axle	Passenger Side Rear Axle	Total Axle Weight
10/98	86-4883	11,400	10,750	11,500	10,600	44,250
	87-4303	11,700	10,400	11,450	10,600	44,150
	87-4308	11,300	11,950	11,850	11,450	46,550
	91-4250	11,850	12,000	12,050	11,800	47,700
						182,650
05/99	86-4883	11,170	11,190	11,150	11,180	44,690
	87-4303	9,410	9,560	9,040	9,560	37,570
	90-4607	10,600	11,490	10,160	11,760	44,010
	91-4250	11,390	12,100	11,150	12,390	47,030
<i>Normalizing Factor for Truck Weight</i>				<i>1.054</i>	173,300	
11/99	87-4308	9,280	9,270	7,770	7,650	33,970
	89-4321	13,800		10,760		24,560
<i>Normalizing Factor for Truck Weight</i>				<i>NA</i>	58,530	
04/00	99-5192	12,490	11,910	11,100	11,320	46,820
	99-5193	9,660	10,790	10,300	10,300	41,050
	87-4308	10,720	10,170	10,690	10,030	41,610
	91-4250	10,680	10,400	10,350	10,060	41,490
<i>Normalizing Factor for Truck Weight</i>				<i>1.0683</i>	170,970	
11/00	91-4250	9,640	9,900	11,860	12,040	43,440
	5067	9,560	9,660	10,400	10,580	40,200
	99-5192	10,080	9,880	11,320	11,540	42,820
	90-4607	9,520	9,840	10,240	10,340	39,940
<i>Normalizing Factor for Truck Weight</i>				<i>1.0977</i>	166,400	
09/02	99-5193	13,520	10,600	11,500	11,140	46,760
	90-4607	11,540	11,660	13,200	12,900	49,300
	00-5067	12,640	12,480	13,680	13,920	52,720
	99-5192	9,960	9,720	11,360	11,340	42,380
<i>Normalizing Factor for Truck Weight</i>				<i>0.9555</i>	191,160	

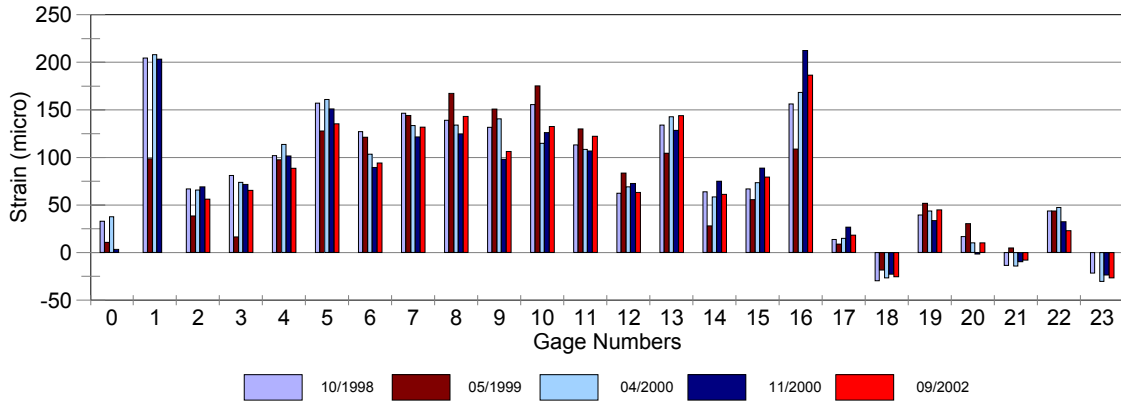


**Figure 8. Strain data under proof loads over four years.**

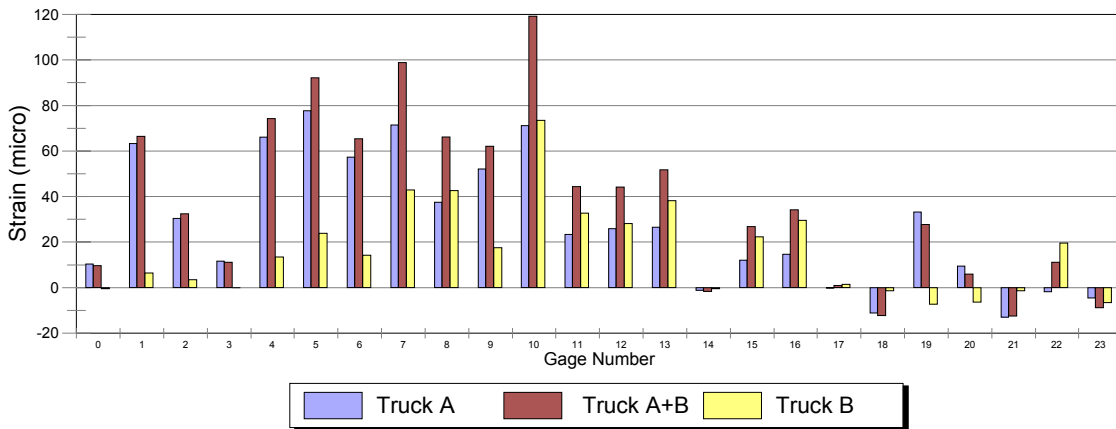


**Figure 9. Strain data under loads during November 1999 tests.**

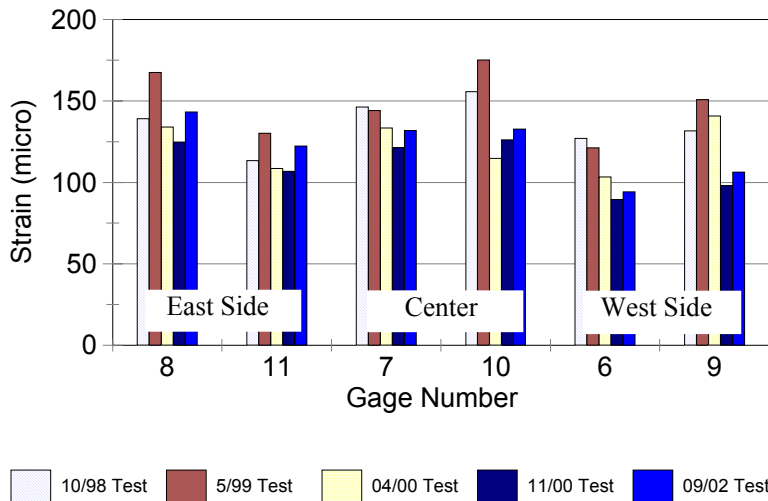


**Figure 10. Strains on both sides of shear-key over the years.**

**Table 5. Strain data under proof loads over four years.**

Gage	0	1	2	3	4	5	6	7	8	9	10	11
10/98	33	204	67	81	102	157	127	146	139	132	156	113
05/99	11	99	38	16	98	128	121	144	167	151	175	130
04/00	38	208	66	74	114	161	103	133	134	141	115	108
11/00	3	191	67	75	110	159	92	126	137	98	132	118
09/02	--	--	56	65	89	135	94	132	143	106	133	122
Gage	12	13	14	15	16	17	18	19	20	21	22	23
10/19	62	134	64	67	156	14	-30	40	17	-14	44	-22
05/19	83	104	28	56	109	9	-18	52	30	5	44	--
04/00	69	143	58	74	168	15	-27	44	10	-14	47	-30
11/00	74	131	83	94	215	35	-21	38	3	7	27	-18
09/02	63	144	61	79	186	18	-26	45	10	-8	23	-27

**Table 6. Stain data under two loaded trucks during November 1999 tests.**

Gage	0	1	2	3	4	5	6	7	8	9	10	11
Truck A	10	63	30	12	66	78	57	72	38	52	71	23
Truck A+B	10	67	32	11	74	92	65	99	66	62	119	44
Truck B	-1	6	3	0	13	24	14	43	43	18	73	33
Gage	12	13	14	15	16	17	18	19	20	21	22	23
Truck A	26	27	-1	12	15	0	-11	33	9	-13	-2	-5
Truck A+B	44	52	-2	27	34	1	-12	28	6	-12	11	-9
Truck B	28	38	-1	22	29	1	-1	-7	-6	-1	20	-7

**Table 7. Strains from gages on either side of the shear-key under proof-loads.**

Gage	8	11	7	10	6	9
10/1998	139	113	146	156	127	132
05/1999	167	130	144	175	121	151
04/2000	134	108	133	115	103	141
11/2000	137	118	126	132	92	98
09/2002	143	122	132	133	94	106

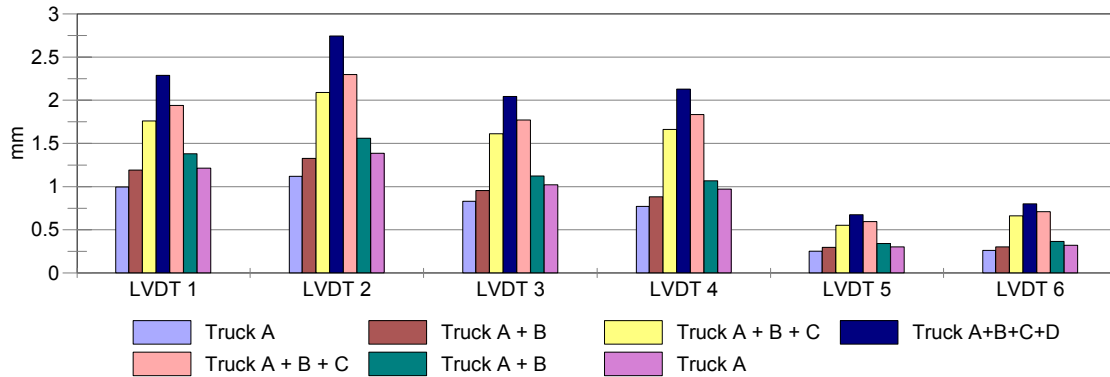


Figure 11. Deflections on both sides of the shear-key during April 2000 load test.

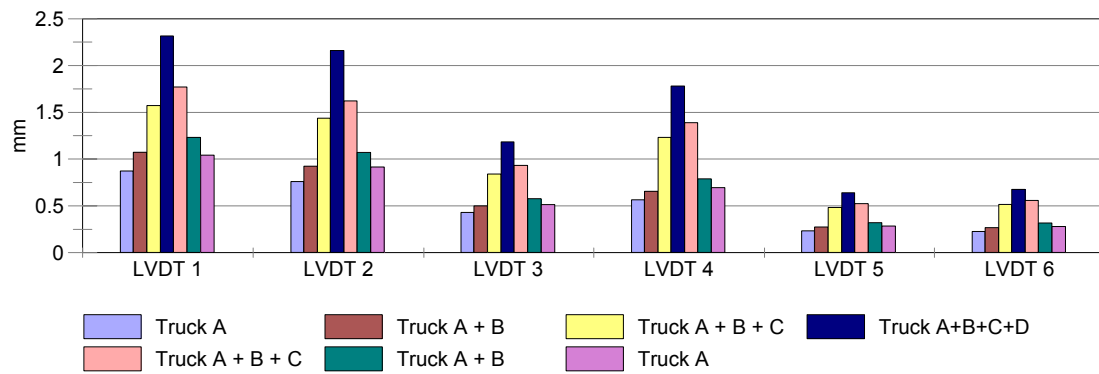


Figure 12. Deflections on both sides of the shear-key during November 2000 load test.

Table 8. Deflections (mm) on both sides of the shear-key during April 2000 load test.

	LVDT 1	LVDT 2	LVDT 3	LVDT 4	LVDT 5	LVDT 6
Truck A	0.996	1.119	0.831	0.770	0.253	0.263
Truck A+B	1.192	1.327	0.954	0.882	0.297	0.301
Truck A+B+C	1.760	2.089	1.613	1.661	0.553	0.663
Truck A+B+C+D	2.288	2.746	2.043	2.129	0.673	0.801
Truck A+B+C	1.940	2.298	1.771	1.835	0.594	0.708
Truck A+B	1.381	1.561	1.122	1.068	0.341	0.364
Truck A	1.215	1.386	1.020	0.971	0.302	0.321

Table 9. Deflections (mm) on both sides of the shear-key during November 2000 load test.

	LVDT 1	LVDT 2	LVDT 3	LVDT 4	LVDT 5	LVDT 6
Truck A	0.873	0.761	0.430	0.564	0.234	0.227
Truck A+B	1.073	0.925	0.500	0.655	0.273	0.266
Truck A+B+C	1.571	1.437	0.839	1.231	0.482	0.517
Truck A+B+C+D	2.316	2.161	1.183	1.781	0.638	0.676
Truck A+B+C	1.770	1.623	0.932	1.388	0.524	0.557
Truck A+B	1.233	1.072	0.578	0.789	0.320	0.318
Truck A	1.043	0.915	0.513	0.695	0.284	0.281

## D. IMPACT FACTORS

AASHTO specifications suggest the amount of impact allowance or increment expressed as a fraction of the live load stresses, and is determined by the formula:

$$I = 50/(L+125)$$

where, I is the impact factor, not to exceed 0.30, and L is the span length in feet. Thus, an impact factor of 0.3 was used in the design of the FRP deck in this project. FRP superstructures are new to civil applications and therefore not much information is available on the impact factors associated with these bridges. Hence, it was decided to measure the impact factors through field testing to verify the assumptions made. Required testing was done during September 2002.

Static response induced by a loaded truck “crawling” across the bridge at about 8km/hr (5 mph) was used as a reference. The same loaded truck was driven across the bridge at the posted speed limit (90 km/hr or 55 mph). The maximum measured response induced by the vehicle was divided by the maximum static response (obtained at crawl speed) to obtain the impact factor. Data was from six different gages and the impact factors varied from 0.06 to 0.52 (see Figure 13 and Table 10). Note that a running average was used to smooth the plots shown in the Figure 13. Consequently, the peak values may appear different than actual peak values reported in Table 10.

## E. DYNAMIC CHARACTERISTICS

Experimental modal analysis techniques were used to characterize dynamic properties of the FRP superstructure and to calibrate theoretical analyses. The calibrated finite element analyses were then used to investigate the use of modal techniques for shear key inspection and damage detection (5). Test results were also used to verify the support fixity and behavior of the longitudinal joint.

An impact test setup was used (6). A total of 37 measurement locations were chosen, such that behavior of the structure in the modes of interest could be represented (Fig. 14). The accelerometer location was chosen so that it was assumed and later verified not to be a modal node within the frequency range of interest. Data were collected in the 0-500 Hz range with 0.3125 Hz frequency resolution. Modal parameters were estimated with global curve-fitting techniques using software from Spectral Dynamics, Inc. Due to the limited number of measurement locations chosen, only the first 8 mode shapes were identified .

The frequency and damping values for the first 8 modes are presented in Table 11 and the mode shapes are shown in Figure 15. The mode shapes exhibited the characteristics of a plate with continuity near the longitudinal joint, confirming the effectiveness of the longitudinal shear-key. The magnitude of the motions at the abutments indicate that the superstructure is well anchored and a near fixed condition exists instead of the simply-supported boundary conditions assumed in the preliminary finite element analysis. The vibration absorbing capacity of FRP superstructure is also reflected in the damping values, which are higher than those for typical steel structures.

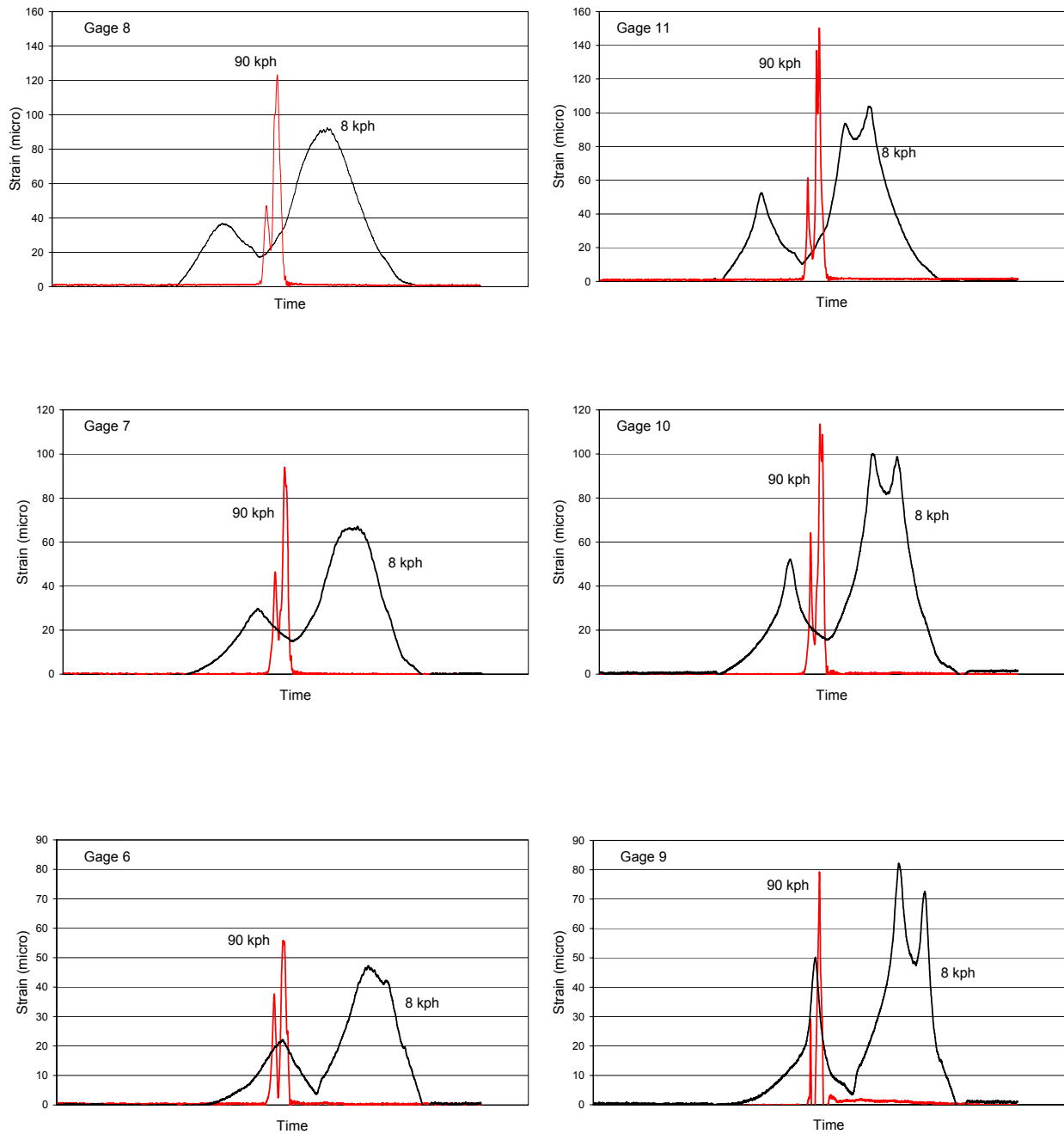


Figure 13. Data from dynamic tests.



**Table 10. Strain data from dynamic tests.**

Gage	Max Strain 90 km/hr	Max Strain 8 km/hr	Impact Factor (I)
6	58	48	0.21
9	89	84	0.06
7	96	68	0.41
10	118	101	0.17
8	125	94	0.33
11	160	105	0.52

**Table 11. Natural Frequencies and Damping Ratios.**

Mode No.	Frequency (Hz)	Damping (%)
1	26.80	4.53
2	29.94	2.11
3	32.07	3.23
4	35.22	2.68
5	41.67	1.73
6	55.46	2.72
7	76.56	2.31
8	90.35	2.56

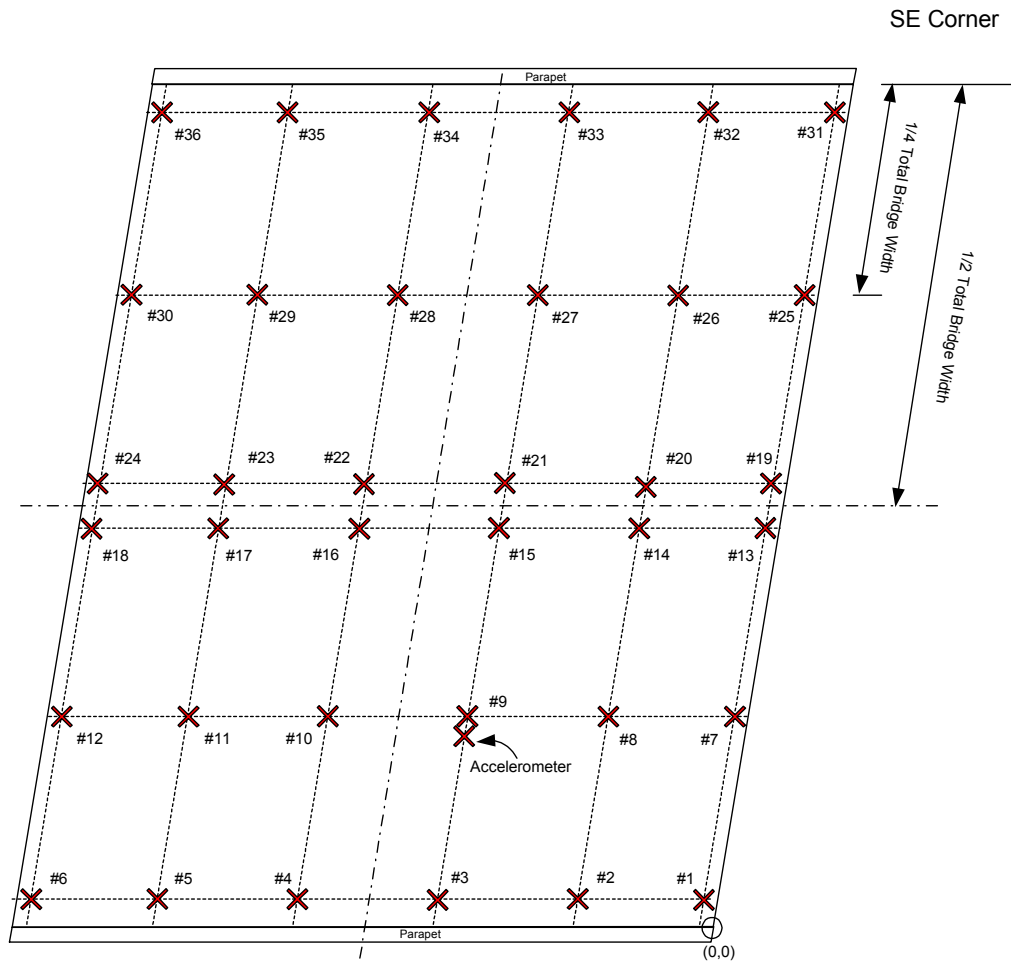


**Figure 14. Plan view of the superstructure showing measurement locations.**

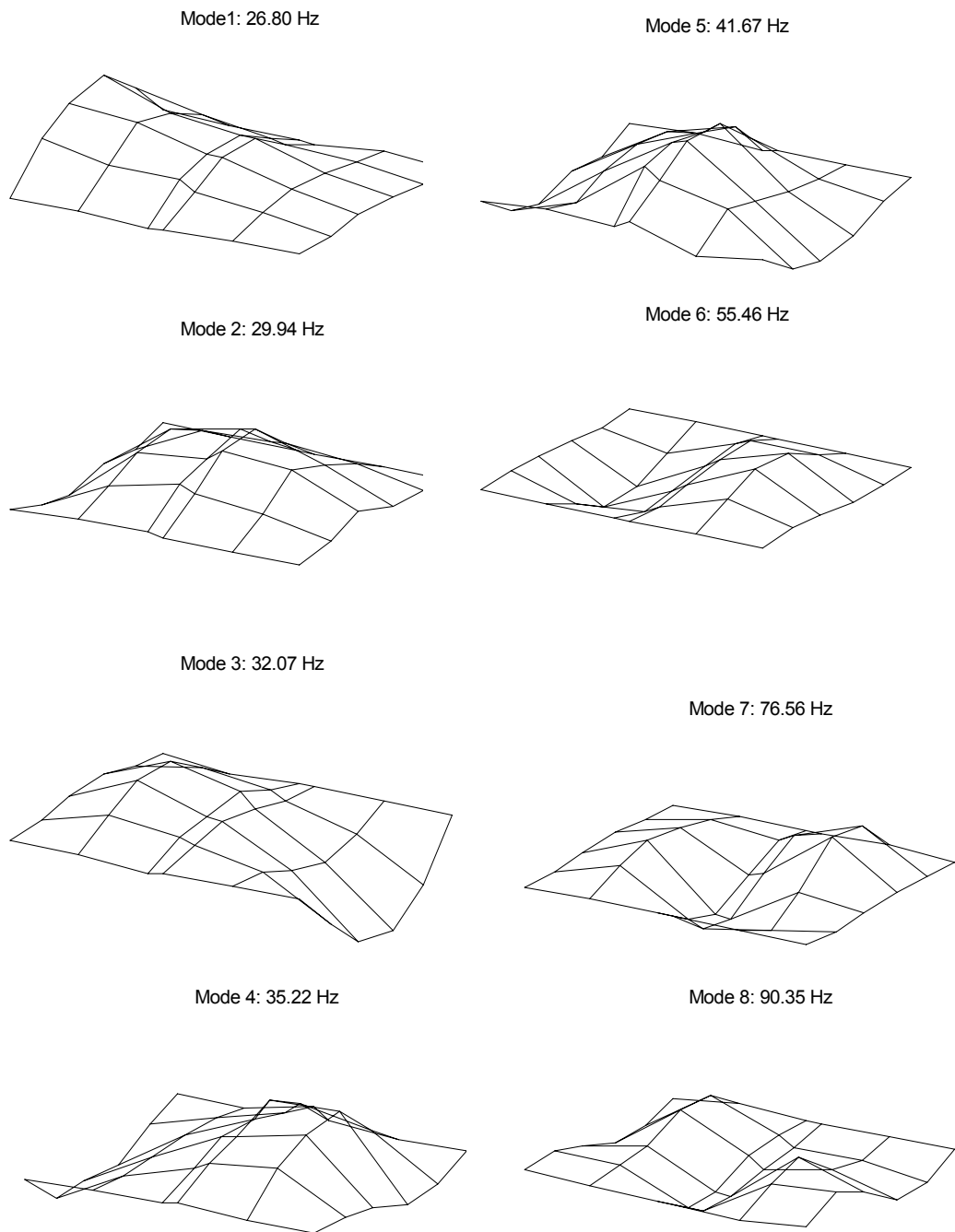


**Figure 15. Mode shapes of the FRP Superstructure.**

## F. VISUAL INSPECTION

In addition to the strain and deflection gage monitoring of the bridge, other in-service monitoring techniques are also being used. The bridge is subject to the general bridge inspection requirements by the National Bridge Inspection Standards (NBIS) for all bridges carrying public highway traffic. This bridge has also been subjected to more frequent, supplemental inspections because of its experimental nature. As most bridge inspectors are unfamiliar with FRP materials, supplemental inspection guidelines have been prepared by Hardcore Composites, LLC, the manufacturer of the superstructure. Particularly, inspectors have been alerted to check for delaminations in the FRP materials. This has been done by tapping the underside of the bridge surface with a rubber mallet. A coin or small rounded stone has proven to be equally effective. A void in the bottom of the deck was discovered soon after placement. The void was repaired in June 2000 by injecting resin.

Monitoring has also included checking for cracks in the FRP materials and any signs of ultraviolet or moisture deterioration. Additionally, the condition of the 10-mm polymer concrete wearing surface has been checked. This has been done by both visual inspection and chain dragging to check for delamination between the polymer concrete and the FRP structure. Some damage to the polymer concrete wearing surface at the bridge ends has been noted. The damage has been attributed to heavy equipment used during approach paving operations or snow plows during the winter. Excessive wear was reported after the first 1.5 years of service. The wearing surface was renewed in June 2000 by applying a broom 'n' seed application of the Transpo T-48 surface after sand blasting the old surface clean. Table 12 gives the notable information from the annual visual inspection reports.

**Table 12. Notable observations from the visual inspection reports.**

Inspection Date	Observations
11/24/98	Three areas of debonding amounting to about 0.15m <sup>2</sup> were observed under the right side slab at midspan.
06/24/99	Top of the deck observes to be breaking up at the junction of the transverse and longitudinal joints. A large portion under the right slab (1/4 to 1/3) has delaminated from midspan to near the end section of the slab.
01/13/00	Wearing surface has been reworked but still has a longitudinal crack at the centerline. Delaminations were repaired by epoxy injection. The slab now sounds solid when sounded with a hammer or stone.
10/22/01	Inspection report shows bottom west side slab showing delaminations again. The repairs to this section of the slab are sound. The delaminations noted appear to be new and require further investigation.
11/13/02	Forty percent of the bottom west side slab seems delaminated when sounded. Repairs to this section of the slab are still sound.

The Infrared Thermography as a means to evaluate the slab integrity is under review. The limitations and sensitivity of this nondestructive test method in detecting the damage in the deck is being explored. A typical picture, of the top surface of the deck, taken using an infrared camera is shown in Figure 16.

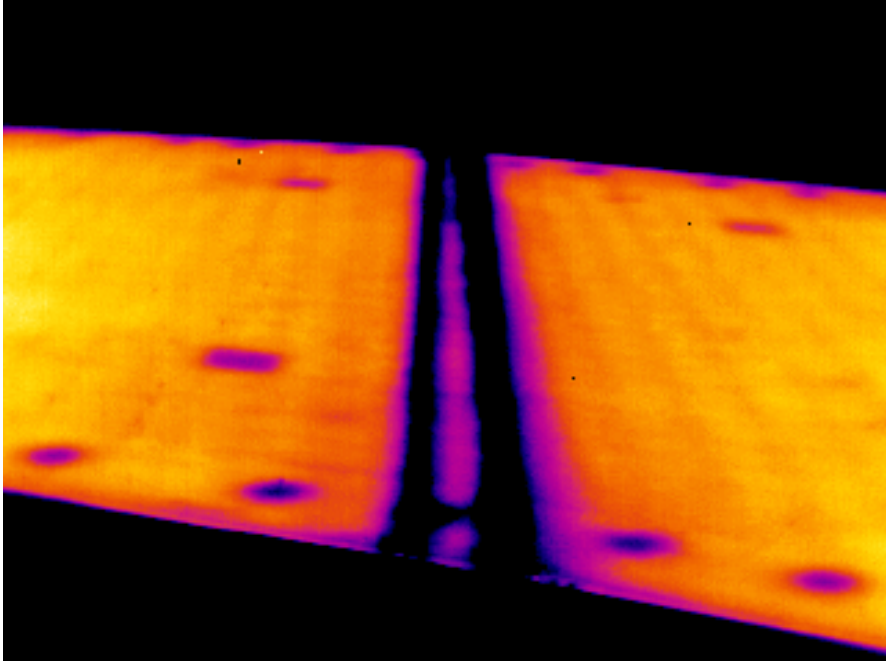


**Figure 16. Infrared photo of the deck top surface.**



#### **IV. CONCLUSIONS**

The first fiber reinforced polymer composite bridge superstructure in New York State was installed in late 1998. This was also the first such bridge to use high skew angle, integral barrier, and deck cross slope. Since durability of the FRP materials for bridge applications is not yet available, the bridge was monitored for its in-service performance before these materials are widely used for such applications in New York State. A detailed test program of periodic testing and visual inspections was used to monitor its in-service performance, characterize its dynamic properties, and obtain data to calibrate theoretical analyses. This report documents the test program and summarizes the results. The test data indicate that the superstructure is structurally performing well. Several delaminations were found during visual inspections. The wearing surface was replaced once. For future applicability of these materials for such applications, these issues affecting the long-term durability of FRP bridge decks should be resolved.





## **ACKNOWLEDGMENTS**

The authors acknowledge the contributions of Department personnel, especially from the Region 6, for their assistance in load testing. Arthur Yannotti, Mark Norfolk, and Jonathan Kunin reviewed the report.



## REFERENCES

1. Alampalli, S., O'Connor, J., and Yannotti, A. "Design, Fabrication, Construction, And Testing of an FRP Superstructure," Transportation Research & Development Bureau, New York State Department of Transportation, Special Report 134, December 2000.
2. "Standard Specifications for Highway Bridges," American Association for Highway and Transportation Officials, 15<sup>th</sup> Edition, Washington, D.C., 1994.
3. "Level 1 Load Rating - BIN 104315022," Report submitted to New York State Department of Transportation by Wagh Engineers, P.C., January 1999.
4. Lichtenstein, A.G. "Bridge Rating Through Nondestructive Load Testing," Technical Report, NCHRP Project 12-28 (13)A, June 1993.
5. Aref, A.J., and Alampalli, S. "Dynamic Behavior and Damage Detection of a Fiber Reinforced Plastic Bridge Structure," ASCE Structures Congress 2000, Philadelphia, PA, May 2000.
6. Ewins, D.J. "Modal Testing: Theory and Practice," John Wiley, New York, 1984.





